

**ANALYSIS OF HIGH FREQUENCY PLANE WAVE
SCATTERING FROM A DOUBLE NEGATIVE
CYLINDER VIA THE MODIFIED WATSON
TRANSFORMATION AND DEBYE EXPANSION**

S. G. Şen

Department of Electrical and Electronics Engineering
Atatürk University
Erzurum 25240, Turkey

M. Kuzuoğlu

Department of Electrical and Electronics Engineering
Middle East Technical University
Ankara 06531, Turkey

Abstract—The modified Watson transform is applied to the Mie series expression of the electromagnetic field scattered by a high frequency plane wave incident on an infinitely long double negative cylinder. The Debye expansion is applied to the Mie series coefficients to obtain a physical insight into the scattering mechanisms and achieve an efficient approach for the computation of the scattered field. The first two terms of the Debye series are computed using the residue series in the geometrical shadow regions and using the steepest descent method in the geometrically lit regions. It is observed that the results obtained from the series and from the modified Watson transform are in good agreement. The angular boundaries for the geometrically lit and the geometrical shadow regions of the double negative cylinder corresponding to the first two terms of the Debye series are determined. These are compared with the corresponding angular boundaries for a double positive cylinder. It is observed that the spatial extent of the geometrical shadow of the double negative cylinder corresponding to the second term of the Debye series is very small compared to that of the double positive cylinder due to the negative refraction in the double negative cylinder when the magnitude of the refractive index n is greater than $\sqrt{2}$.

1. INTRODUCTION

Double negative or left handed metamaterials are the artificial realizations of the theoretical material presented in the article [1] of Veselago in 1968. Veselago theoretically examined the properties of a material with a negative permittivity and a negative permeability. Due to having both negative parameters, these materials are called double negative metamaterials. In the studies made for the realization of the double negative metamaterials, the articles [2] and [3] are often referred. [2] and [3] are the fundamental articles for the SRR and thin-wire realizations of left-handed metamaterials. In [4–6], the construction of double negative metamaterials, the numerical and experimental verification of double negativeness and negative refraction are reported. [7, 8] examine the propagation of electromagnetic waves through double negative metamaterials especially in terms of causality using FDTD method. A popular realization of double negative metamaterials which is the L-C loaded transmission line approach is introduced, numerically and experimentally demonstrated in [9–12]. [13–15] report experimental and numerical studies about the electromagnetic wave propagation through double negative metamaterials. Double negative metamaterials have also practical applications. Some of them are given in [16–24]. The scattering of electromagnetic waves from DNG multilayered cylinders are studied in [25–31]. [32, 33] give a review of the research on double negative metamaterials.

The expression of the scattered field due to a plane wave incident on an infinitely long dielectric cylinder can be obtained via a Mie series expansion. When the diameter of the dielectric cylinder is much larger than the wavelength of the incident plane wave, the Mie series expansion converges slowly. Apart from this slow convergence behavior which increases the computational burden, the Mie series expansion does not provide any physical insight into the scattering mechanisms. These difficulties may be overcome by applying the modified Watson transform with the Debye expansion of the scattering coefficients in the Mie series expansion. Following this approach, the convergence of the Debye terms of the scattered field and the scattered field becomes faster, and it becomes possible to identify certain scattering mechanisms. The first use of the Watson transform is in [35] by Watson. Some other realizations of the Watson transform are given in [36–43]. The Debye expansion is first introduced and applied by Debye in his work [34] for examining the scattering by a dielectric cylinder. Some applications of the Debye expansion are given in [40–43]. The Debye expansion along with the modified Watson

transform is used in [40] and [41] for analyzing the scattering from infinitely long dielectric cylinders. In all of these works, the dielectric cylinders are double positive, i.e., the permittivity and permeability parameters are positive constants. In [42], the Debye expansion is applied to calculate the scattering amplitude of a scalar wave from a penetrable sphere. In [43], the scattering of a scalar plane wave from an impenetrable sphere is analyzed using the modified Watson transform. The approaches used in articles [42] and [43] are employed in this paper to use the modified Watson transform along with Debye expansion for the analysis of scattering from double negative and double positive infinitely long cylinders. Double negative metamaterials are artificially obtained materials with negative permeability and permittivity. Due to the causality requirements, double negative metamaterials have negative refractive indices. The main goal of this paper is to derive and compare the results of scattering from double positive and double negative dielectric cylinders. The outline of the paper is as follows: In the second section, the Mie series expansions of the scattered fields from double positive and double negative infinitely long cylinders are derived. In the third section, the modified Watson transform is applied to the Mie series form of the scattered field. The poles of the modified Watson transform integrand are examined. The need for applying the Debye expansion to the scattering coefficients is indicated. In the fourth section, the Debye expansion is applied to the scattering coefficients. The physical meaning of the Debye expansion is explained. In the fifth and the sixth sections, the physical “ray” pictures for the first two terms of the Debye expansions for the scattered fields from double negative and double positive cylinders are drawn. The geometrical shadow and the geometrically lit regions of the first two terms of the Debye series for the double positive and double negative cylinders are determined. The validity of the physical pictures is proven using the saddle point method and the residue series calculations. Further verification is made comparing the series results for the first two terms of the Debye expansion with the SDM results and the residue series calculations in section seven. The conclusions of this work are presented in the eighth section.

2. THE MIE SERIES EXPANSION FOR THE SCATTERED FIELD

Assuming a time-harmonic dependence of $e^{-j\omega t}$, a plane wave

$$\vec{E}^i = \hat{a}_z e^{-jk_0 x} \quad (1)$$

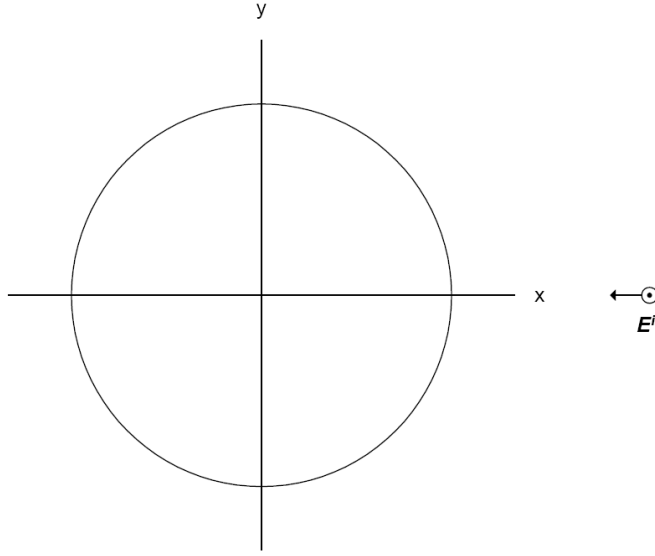


Figure 1. The problem geometry.

propagates in the negative x direction where

$$k_0 = \omega \sqrt{\mu_0 \epsilon_0} \quad (2)$$

is the free space propagation constant. As shown in Fig. 1, the center of the cross-section of a dielectric circular cylinder of infinite length is located at the origin. The cylinder radius is a and it is assumed to be much larger than the wavelength of the incident plane wave. The incident plane wave is expressed as a series employing Bessel functions of the first kind as follows:

$$\vec{E}^i = \hat{a}_z \sum_{l=-\infty}^{\infty} j^{-l} J_l(k_0 \rho) e^{jl\phi} \quad (3)$$

The scattered field at the field point $P(\rho, \phi)$ can be written in terms of a series of Hankel functions of the first kind:

$$\vec{E}^s = \hat{a}_z \sum_{l=-\infty}^{\infty} c_l H_l^{(1)}(k_0 \rho) e^{jl\phi} \quad (4)$$

After satisfying the continuity of the tangential electric field intensity and the tangential magnetic field intensity at the surface of the double

positive cylinder, the following expression is obtained for c_l :

$$c_l = \frac{j^{-l}[-\mu_r J_l(\alpha) J_l'(\beta) + n J_l'(\alpha) J_l(\beta)]}{[\mu_r J_l(\alpha) H_l^{(1)'}(\beta) - n J_l'(\alpha) H_l^{(1)}(\beta)]} \quad (5)$$

where the positive μ_r is the relative permeability of the cylinder, the positive n is the refractive index of the double positive cylinder, and

$$\beta = k_0 a \quad (6)$$

$$\alpha = n\beta \quad (7)$$

The convention for $f'(x_0)$ is given as follows:

$$f'(x_0) = \left. \frac{df}{dx} \right|_{x=x_0} \quad (8)$$

The Equation (4) is the Mie series solution for the scattered field. The scattering coefficients for a double negative cylinder are obtained inserting the following relations into the expression in Equation (5):

$$\begin{aligned} \alpha &= -|n|\beta \\ J_l(\alpha) &= e^{j\pi l} J_l(|n|\beta) \\ J_l'(\alpha) &= (-1)^l e^{j\pi l} J_l'(|n|\beta) \end{aligned} \quad (9)$$

The scattering coefficients c_l for a double negative infinitely long cylinder with a relative permeability $-\mu_r$ and a refractive index of $-|n|$ are given by the following:

$$c_l = \frac{j^{-l} [|\mu_r| J_l(|n|\beta) J_l'(\beta) + |n| J_l'(|n|\beta) J_l(\beta)]}{[-|\mu_r| J_l(|n|\beta) H_l^{(1)'}(\beta) - |n| J_l'(|n|\beta) H_l^{(1)}(\beta)]} \quad (10)$$

As an illustration of the slow convergence of the Mie series form of the scattered field, the number of terms to be kept in the Mie series for the correct result is shown versus β values in Fig. 2 obtained using Mathematica. It can be observed that the number of terms to be kept in the sum must be at least approximately the integer closest to 2β . The results are for the scattering from a dielectric cylinder of the refractive index 3 and relative permeability 1. The ϕ coordinate of the field point is π radian and the ρ coordinate is $3(\beta + \beta^{\frac{1}{3}})$.

3. THE MODIFIED WATSON TRANSFORM

The modified Watson transform is an approach for obtaining a rapidly converging solution with physical insight into the scattering

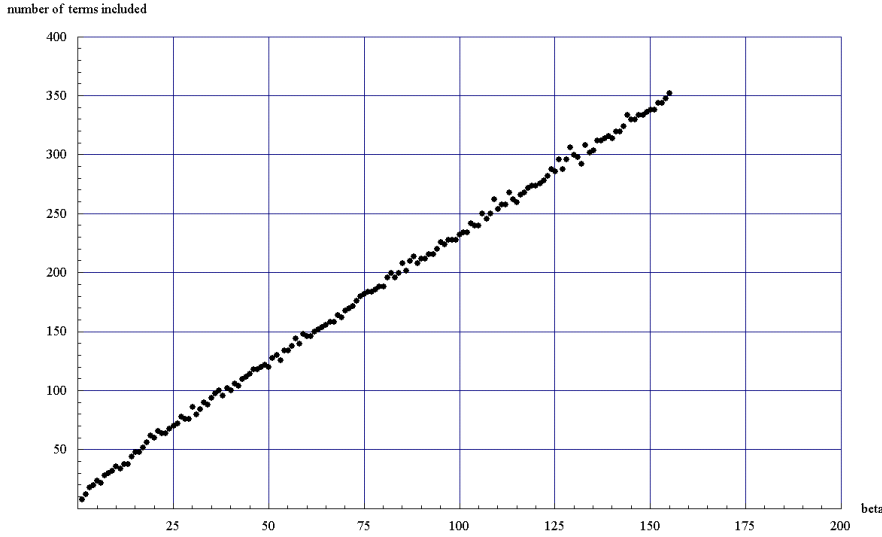


Figure 2. The number of terms to be kept in the Mie series versus beta for the convergence of the Mie series.

mechanism. After the application of the modified Watson transform to the Mie series form of the scattered field at the field point $P(\rho, -\phi)$ which is the same as the field at the field point $P(\rho, \phi)$ due to the symmetry of the problem, the scattered field can be written as follows:

$$E^s = -\frac{1}{2j} \int_{-\infty+j\varepsilon}^{\infty+j\varepsilon} \left[c_{-\nu} H_{-\nu}^{(1)}(k_0\rho) e^{j\nu(\phi-\pi)} + c_{\nu} H_{\nu}^{(1)}(k_0\rho) e^{-j\nu(\phi-\pi)} \right] \left[2 \sum_{m=0}^{\infty} (-1)^m e^{j(2m+1)\pi(\nu-\frac{1}{2})} \right] d\nu \quad (11)$$

One of the methods to calculate the integral in (11) for the scattered field is to use the Cauchy integral formula. For this method, the poles of the integrand in the upper half of the complex ν -plane must be examined. The integral in Equation (11) consists of two parts. The first part is

$$-\frac{1}{2j} \int_{-\infty+j\varepsilon}^{\infty+j\varepsilon} \left[c_{-\nu} H_{-\nu}^{(1)}(k_0\rho) e^{j\nu(\phi-\pi)} \right] \left[2 \sum_{m=0}^{\infty} (-1)^m e^{j(2m+1)\pi(\nu-\frac{1}{2})} \right] d\nu \quad (12)$$

and the second part is

$$-\frac{1}{2j} \int_{-\infty+j\varepsilon}^{\infty+j\varepsilon} \left[c_\nu H_\nu^{(1)}(k_0\rho) e^{-j\nu(\phi-\pi)} \right] \left[2 \sum_{m=0}^{\infty} (-1)^m e^{j(2m+1)\pi(\nu-\frac{1}{2})} \right] d\nu \quad (13)$$

The poles of the second part are the poles of c_ν given by

$$c_\nu = \frac{j^{-\nu} [-\mu_r J_\nu(\alpha) J'_\nu(\beta) + n J'_\nu(\alpha) J_\nu(\beta)]}{[\mu_r J_\nu(\alpha) H_\nu^{(1)'}(\beta) - n J'_\nu(\alpha) H_\nu^{(1)}(\beta)]} \quad (14)$$

At this point we introduce some notations taken from [42] for the easy handling of equations with Bessel and Hankel functions:

$$[x] \triangleq \frac{J'_\nu(x)}{J_\nu(x)} \quad [1x] \triangleq \frac{H_\nu^{(1)'}(x)}{H_\nu^{(1)}(x)} \quad [2x] \triangleq \frac{H_\nu^{(2)'}(x)}{H_\nu^{(2)}(x)} \quad (15)$$

The poles of c_ν are actually the roots of

$$\mu_r J_\nu(\alpha) H_\nu^{(1)'}(\beta) - n J'_\nu(\alpha) H_\nu^{(1)}(\beta) = 0 \quad (16)$$

Using the notations given above, Equation (16) can be written in a compact form:

$$[1\beta] = \frac{n}{\mu_r} [\alpha] \quad (17)$$

The roots of Equation (17) can be divided into two groups. One group consists of those which are almost parallel to the real ν -axis. There are an infinite number of these roots. The other group contains those which are almost parallel to the imaginary ν -axis. The poles of the integrand are shown in Fig. 3.

For the calculation of the integral (13), the residues of the integrand at these two groups of poles are computed and summed up. Since the residues at the poles which are almost parallel to the imaginary ν -axis are rapidly decaying exponentials, these poles make a quickly vanishing contribution and provide a quickly converging result. However, the poles which are almost parallel to the real ν -axis cause a difficulty in the computation. The contribution of their residues does not vanish quickly. Hence, the residue series of these poles does not converge rapidly. Due to such a poor convergence property, calculating the integral (13) using the Cauchy integral formula is not an efficient method. The integral (12) is similar to the integral (13). Hence, in addition to the modified Watson transformation, some more modifications must be made to the modified Watson transform form of the scattered field. These modifications are collected under the title of Debye expansion.

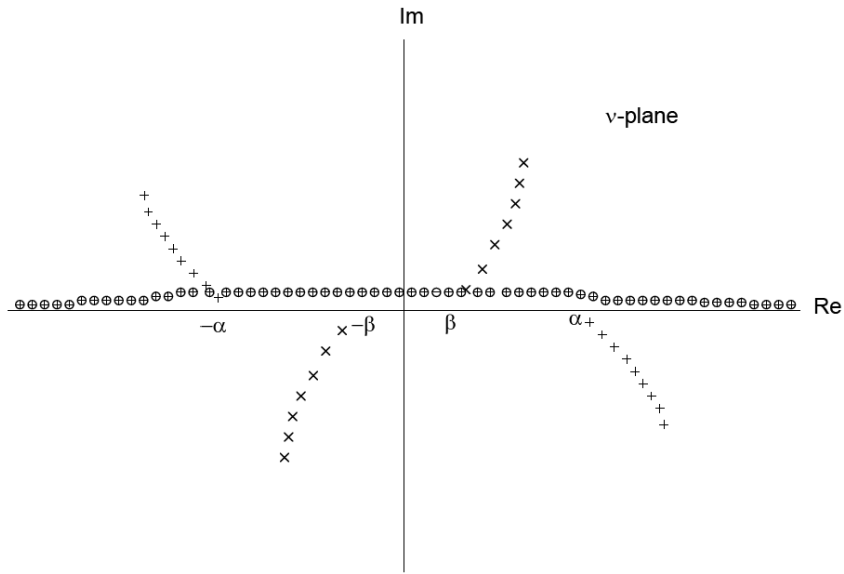


Figure 3. The roots of Equation (17).

4. THE DEBYE EXPANSION

For high frequency applications, the incident plane wave can be modeled to be made up of incident rays. Each ray incident on the dielectric cylinder is reflected and refracted by the cylinder. However, the reflection and refraction occur infinitely many times. Let a ray be followed in this series after it is incident to the surface of the cylinder. Some part of it is reflected and the rest is transmitted into the cylinder by refraction. The reflection of the ray to the outside of the cylinder is called the first term in the series. This reflected part contributes to the scattered field as the first term. The transmitted part of the ray travels in the cylinder and hits the surface from inside. Then, part of it is reflected and part of it is transmitted to the outside. This transmitted part forms the second term in the series and it contributes to the scattered field as the second term in the series. The third term in the series is the part of the ray which is obtained after the first transmission into the cylinder, then reflection from inside the cylinder, and then transmission to the outside of the dielectric cylinder. The mentioned scattering mechanism is pictured in Fig. 4. The series is built up in this way and converges to the scattered field at the end.

At high frequency, the physical picture in Fig. 4 can be employed for the problem. This physical picture is used for the scattering

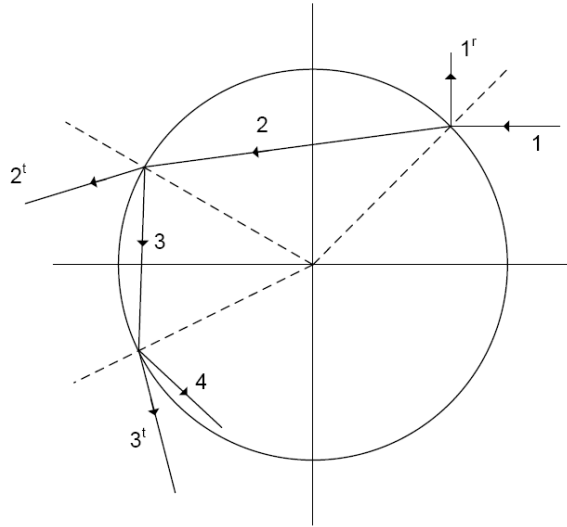


Figure 4. The scattering mechanism at high frequency.

amplitude calculation due to a penetrable sphere in [42], for calculation of the scattered wave function of an impenetrable sphere in [43]. A similar mathematical and a physical framework can be constructed for the scattering by a dielectric cylinder. The scattered field is a series of Hankel functions of the first kind scaled by the scattering coefficients c_l . The scattering field coefficients take their final forms after the series of reflections and transmissions of cylindrical waves. This implies that the coefficients c_l form the mathematical representation of the scattering phenomenon given in Fig. 4 and must contain the overall related mathematical information. The physical picture in Fig. 4 is mathematically expressed in [42] by decomposing a quantity called S -function into a series of reflection and transmission terms shown in Fig. 4. Depending on this information and the fact that the scattering coefficients c_l must contain the overall information about Fig. 4, it is concluded that c_l must be able to be written in terms of the S -function which is denoted as x_l in this analysis and given in Equation (18). By expressing c_l in terms of x_l , c_l is decomposed into the mathematical building blocks of the whole physical picture and the Debye expansion is carried out.

Since the scattering object is a cylinder, using the cylindrical coordinates and expressing each ray in terms of cylindrical functions is the most appropriate choice. Each incident ray can be written as a series of a linear combination of Hankel functions of first and second

kinds. These linear combinations of Hankel functions are reflected and transmitted in an infinite sequence to obtain the scattered field. The reflection and transmission coefficients in x_l are defined considering the just mentioned scattering mechanism. x_l is defined as follows:

$$x_l = \frac{H_l^{(2)}(\beta)}{H_l^{(1)}(\beta)} \left\{ R_{22}(l, \beta) + T_{21}(l, \beta) T_{12}(l, \beta) \frac{H_l^{(1)}(\alpha)}{H_l^{(2)}(\alpha)} \sum_{p=1}^{\infty} \left[R_{11}(l, \beta) \frac{H_l^{(1)}(\alpha)}{H_l^{(2)}(\alpha)} \right]^{p-1} \right\} \quad (18)$$

where

$$\left| R_{11}(l, \beta) \frac{H_l^{(1)}(\alpha)}{H_l^{(2)}(\alpha)} \right| < 1$$

In Equation (18), $R_{11}(l, \beta)$ is the reflection coefficient for the cylindrical wave which is denoted by the Hankel function of the first kind and is incident from inside of the cylinder to the surface. $R_{22}(l, \beta)$ is the reflection coefficient for the cylindrical wave which is denoted by the Hankel function of the second kind and is incident from outside of the cylinder to the surface. $T_{12}(l, \beta)$ is the transmission coefficient for the cylindrical wave which is denoted by the Hankel function of the first kind and is incident from inside of the cylinder to the surface. $T_{21}(l, \beta)$ is the transmission coefficient for the cylindrical wave which is denoted by the Hankel function of the second kind and is incident from outside of the cylinder to the surface. The mathematical expressions for these coefficients are as follows:

$$R_{11}(l, \beta) = -\frac{[1\beta] - \frac{n}{\mu_r}[1\alpha]}{[1\beta] - \frac{n}{\mu_r}[2\alpha]} \quad R_{22}(l, \beta) = -\frac{[2\beta] - \frac{n}{\mu_r}[2\alpha]}{[1\beta] - \frac{n}{\mu_r}[2\alpha]} \quad (19)$$

$$T_{12}(l, \beta) = \frac{4j}{\pi\beta H_l^{(1)}(\alpha) H_l^{(2)}(\alpha) \left([1\beta] - \frac{n}{\mu_r}[2\alpha] \right)}$$

$$T_{21}(l, \beta) = \frac{4j}{\pi\beta H_l^{(1)}(\beta) H_l^{(2)}(\beta) \left([1\beta] - \frac{n}{\mu_r}[2\alpha] \right)} \quad (20)$$

The first part of x_l which is given by

$$\frac{H_l^{(2)}(\beta)}{H_l^{(1)}(\beta)} R_{22}(l, \beta) \quad (21)$$

corresponds to the rays which are reflected by the cylinder. The rest of it given by

$$\frac{H_l^{(2)}(\beta)}{H_l^{(1)}(\beta)} T_{21}(l, \beta) T_{12}(l, \beta) \frac{H_l^{(1)}(\alpha)}{H_l^{(2)}(\alpha)} \sum_{p=1}^{\infty} \left[R_{11}(l, \beta) \frac{H_l^{(1)}(\alpha)}{H_l^{(2)}(\alpha)} \right]^{p-1} \quad (22)$$

corresponds to the rays which are first transmitted into the cylinder, make $p - 1$ number of reflections and are transmitted to the outside of the cylinder after these $p - 1$ reflections. The scattering coefficients c_l can be written in terms of x_l as follows:

$$c_l = \frac{j^{-l}}{2} (x_l - 1) \quad (23)$$

After writing c_ν in terms of x_ν in Equation (11), the following expression for the scattered field is obtained:

$$\begin{aligned} E^s = & -\frac{1}{2j} \int_{-\infty+j\varepsilon}^{\infty+j\varepsilon} \left[\frac{j^\nu}{2} (x_{-\nu} - 1) H_{-\nu}^{(1)}(k_0\rho) e^{j\nu(\phi-\pi)} \right. \\ & \left. + \frac{j^{-\nu}}{2} (x_\nu - 1) H_\nu^{(1)}(k_0\rho) e^{-j\nu(\phi-\pi)} \right] \\ & \times \left[2 \sum_{m=0}^{\infty} (-1)^m e^{j(2m+1)\pi(\nu-\frac{1}{2})} \right] d\nu \quad (24) \end{aligned}$$

By writing c_ν in terms of x_ν , the expansion called the Debye expansion is applied to c_ν . Through the use of the Debye expansion, the physical mechanism in the scattering is revealed. In addition, the calculation of the integral in (24) using the residue calculus is now preferable and the resulting residue series converges very quickly in the appropriate field region. The reason of the rapid convergence is due to the new denominator of the integrands in (24). The new equation to be solved to find the poles is

$$[1\beta] = \frac{n}{\mu_r} [2\alpha] \quad (25)$$

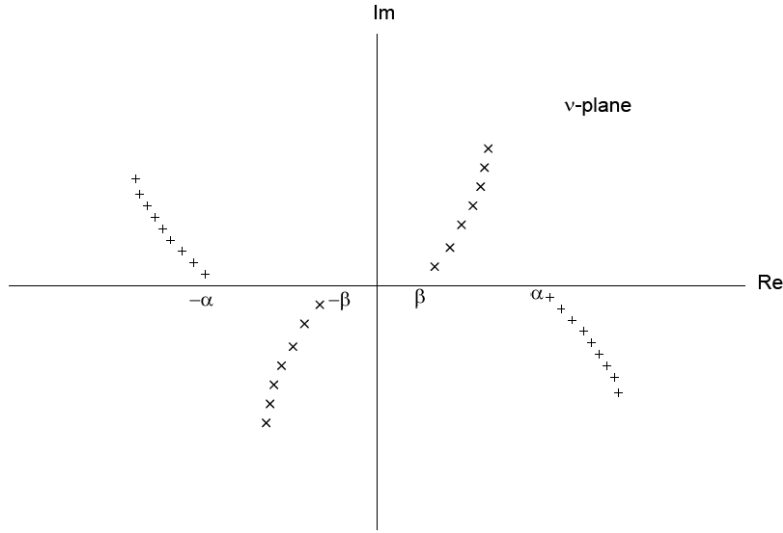


Figure 5. The roots of Equation (25).

Equation (25) is the counterpart of Equation (17). The roots of these equation (i.e., the poles of the integrand) are complex numbers which are almost parallel to the imaginary ν -axis. Now, there are no poles which are almost parallel to the real ν -axis. Hence, the residue series is now quickly convergent. The new poles are shown in Fig. 5.

5. THE FIRST TERM OF THE DEBYE EXPANSION

The contribution of the first term of the Debye expansion to the scattered field is obtained by inserting the expression in (21) with the subscript changed to ν into the place of x_ν in the scattered field integral in (24):

$$\begin{aligned}
 E_{first\ term}^s = & -\frac{1}{2j} \int_{-\infty+j\varepsilon}^{\infty+j\varepsilon} \left[\left[\frac{H_{-\nu}^{(2)}(\beta)}{H_{-\nu}^{(1)}(\beta)} R_{22}(-\nu, \beta) - 1 \right] H_{-\nu}^{(1)}(k_0\rho) e^{j\nu(\phi-\frac{\pi}{2})} \right. \\
 & + \left. \left[\frac{H_{\nu}^{(2)}(\beta)}{H_{\nu}^{(1)}(\beta)} R_{22}(\nu, \beta) - 1 \right] H_{\nu}^{(1)}(k_0\rho) e^{-j\nu(\phi-\frac{\pi}{2})} \right] \\
 & \times \left[\sum_{m=0}^{\infty} (-1)^m e^{j(2m+1)\pi(\nu-\frac{1}{2})} \right] d\nu \quad (26)
 \end{aligned}$$

The integral in (26) is to be calculated using the Cauchy integral formula. For applying the Cauchy integral formula, the integrand of the integral must vanish as $|\nu| \rightarrow \infty$ in the upper half of the complex ν -plane. The current form of the integrand is not suitable for applying the Cauchy integral formula. After addition and subtraction of some appropriate terms, the following integral is obtained:

$$E_{first\ term}^s = \sum_{m=0}^{\infty} \left[\left(-\frac{1}{2j} \right) \left[\int_{-\infty+j\varepsilon}^{\infty+j\varepsilon} I_1(-1)^m e^{-j(2m+1)\frac{\pi}{2}} d\nu \right] + \left(-\frac{1}{2j} \right) \left[\int_{-\infty+j\varepsilon}^{\infty+j\varepsilon} I_2(-1)^m e^{-j(2m+1)\frac{\pi}{2}} d\nu \right] \right] \quad (27)$$

where

$$I_1 = \left[\frac{R_{22}H_{-\nu}^{(2)}(\beta)H_{-\nu}^{(1)}(k_0\rho) + H_{-\nu}^{(1)}(\beta)H_{-\nu}^{(2)}(k_0\rho)}{H_{-\nu}^{(1)}(\beta)} \right] e^{j\nu[\phi - \frac{\pi}{2} + (2m+1)\pi]} + \left[\frac{R_{22}H_{\nu}^{(2)}(\beta)H_{\nu}^{(1)}(k_0\rho) + H_{\nu}^{(1)}(\beta)H_{\nu}^{(2)}(k_0\rho)}{H_{\nu}^{(1)}(\beta)} \right] e^{-j\nu[\phi - \frac{\pi}{2} - (2m+1)\pi]} \quad (28)$$

$$I_2 = - \left[H_{-\nu}^{(1)}(k_0\rho) + H_{-\nu}^{(2)}(k_0\rho) \right] e^{j\nu[\phi - \frac{\pi}{2} + (2m+1)\pi]} + (-1) \left[H_{\nu}^{(1)}(k_0\rho) + H_{\nu}^{(2)}(k_0\rho) \right] e^{-j\nu[\phi - \frac{\pi}{2} - (2m+1)\pi]} \quad (29)$$

The decomposition of the integral in (27) into the integrals of I_1 and I_2 is possible only if each of the integrals of I_1 and I_2 are convergent.

The residue series representation of the integral of I_1 in (27) is given by the following

$$\begin{aligned} & \sum_{m=0}^{\infty} \left[\left(-\frac{1}{2j} \right) \left[\int_{-\infty+j\varepsilon}^{\infty+j\varepsilon} I_1(-1)^m e^{-j(2m+1)\frac{\pi}{2}} d\nu \right] \right] \\ &= \sum_{m=0}^{\infty} \left(-\frac{1}{2j} \right) (2\pi j) \sum_{q=1}^{\infty} \text{Res} \left\{ I_1(-1)^m e^{-j(2m+1)\frac{\pi}{2}} \right\} \Big|_{\nu=\nu_q} \\ &= \sum_{m=0}^{\infty} (-\pi) \sum_{q=1}^{\infty} \left[(-1)^m e^{-j(2m+1)\frac{\pi}{2}} \right] \end{aligned}$$

$$\frac{4jH_\nu^{(1)}(k_0\rho)\left\{e^{j\nu\left[\phi-\frac{3\pi}{2}+(2m+1)\pi\right]}+e^{-j\nu\left[\phi-\frac{\pi}{2}-(2m+1)\pi\right]}\right\}}{\pi\beta[H_\nu^{(1)}(\beta)]^2\frac{\partial}{\partial\nu}\left([1\beta]-\frac{n}{\mu_r}[2\alpha]\right)}\Big|_{\nu=\nu_q} \quad (30)$$

where $\nu = \nu_q$ are the poles of the integrand I_1 . The expression in (30) is for a double positive infinitely long cylinder. The convergence of the residue series in (30) depends on the exponential term. In order to obtain a good approximation to the residue series convergence region which is in agreement with the physical insight to the problem, the Debye asymptotic expansion of $H_\nu^{(1)}(k_0\rho)$ is employed in the residue series. The Debye asymptotic expansion taken from the Appendix A of [43] is given by

$$H_\nu^{(1)}(z) \approx \left(\frac{2}{\pi}\right)^{\frac{1}{2}} (z^2 - \nu^2)^{-\frac{1}{4}} \exp\left\{j\left[(z^2 - \nu^2)^{\frac{1}{2}} - \nu \cos^{-1}\left(\frac{\nu}{z}\right) - \frac{\pi}{4}\right]\right\} \quad (31)$$

with the following expansion conditions

$$\begin{aligned} (z^2 - \nu^2)^{-\frac{1}{4}} > 0 & \quad 0 < \cos^{-1}\left(\frac{\nu}{z}\right) < \frac{\pi}{2} \\ -z < \nu < z & \quad |\nu - z| > |z|^{\frac{1}{3}} \end{aligned} \quad (32)$$

After the insertion of the asymptotic expansion to the residue series in (30), the overall exponential term in the residue series becomes the following

$$\begin{aligned} & \exp\left\{j\left[\left((k_0\rho)^2 - \nu^2\right)^{\frac{1}{2}} - \nu \cos^{-1}\left(\frac{\nu}{k_0\rho}\right) - \frac{\pi}{4} + \nu\left[\phi - \frac{3\pi}{2} + (2m+1)\pi\right]\right]\right\} \\ & + \exp\left\{j\left[\left((k_0\rho)^2 - \nu^2\right)^{\frac{1}{2}} - \nu \cos^{-1}\left(\frac{\nu}{k_0\rho}\right) - \frac{\pi}{4} - \nu\left[\phi - \frac{\pi}{2} - (2m+1)\pi\right]\right]\right\} \end{aligned} \quad (33)$$

Due to the exponential dependence of the residue series on the poles, as the imaginary part of the poles increases, the residue series terms exponentially decay to zero. Hence, the poles far away from the real axis have a negligible effect. Then, the poles of the integrand can be approximated by β . Substituting this approximation into (33), the range of ϕ for the convergence of the residue series is obtained as

follows:

$$\left. \begin{aligned} \frac{\pi}{2} + \cos^{-1}\left(\frac{a}{\rho}\right) < \phi < \frac{3\pi}{2} - \cos^{-1}\left(\frac{a}{\rho}\right) & \text{ for } m = 0 \\ \frac{\pi}{2} + \cos^{-1}\left(\frac{a}{\rho}\right) - 2m\pi < \phi < \frac{3\pi}{2} - \cos^{-1}\left(\frac{a}{\rho}\right) + 2m\pi & \text{ for } m > 0 \end{aligned} \right\} \quad (34)$$

The first part of the information given in (34) for $m = 0$ restricts ϕ to the region called the geometrical shadow region of the dielectric cylinder. The geometrical shadow region of the dielectric cylinder is shown in Fig. 6. The following definition is made for ϕ_0 :

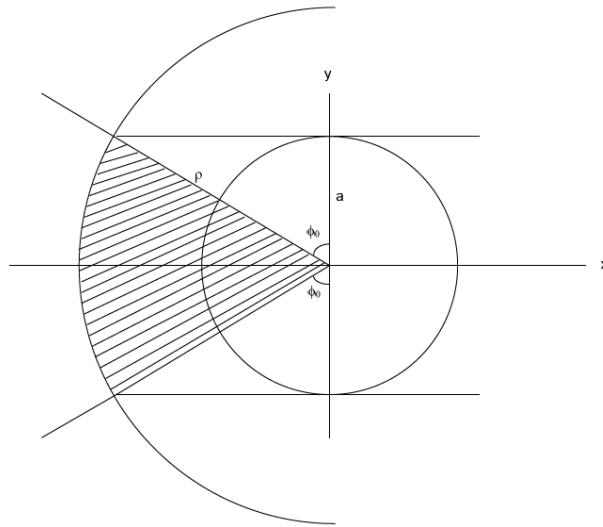


Figure 6. The geometrical shadow region of the double positive cylinder corresponding to the first term of the Debye series.

$$\phi_0 = \cos^{-1}\left(\frac{a}{\rho}\right) \quad (35)$$

For $m > 0$, the range of ϕ covers the whole dielectric cylinder. Hence, the convergence region of the residue series is the geometrical shadow of the dielectric cylinder. The equality in (30) is valid in the geometrical shadow region of the cylinder for the high frequency scattering.

If the infinitely long cylinder is double negative, then the refractive index, the relative permeability and the relative permittivity of the

cylinder will be negative. The field in the geometrical shadow region of the double negative cylinder will be given by

$$\begin{aligned}
& \sum_{m=0}^{\infty} \left[\left(-\frac{1}{2j} \right) \left[\int_{-\infty+j\varepsilon}^{\infty+j\varepsilon} I_1(-1)^m e^{-j(2m+1)\frac{\pi}{2}} d\nu \right] \right] \\
&= \sum_{m=0}^{\infty} \left(-\frac{1}{2j} \right) (2\pi j) \sum_{q=1}^{\infty} \text{Res} \left\{ I_1(-1)^m e^{-j(2m+1)\frac{\pi}{2}} \right\} \Big|_{\nu=\nu_q} \\
&= \sum_{m=0}^{\infty} (-\pi) \sum_{q=1}^{\infty} \left[(-1)^m e^{-j(2m+1)\frac{\pi}{2}} \right] \\
& \quad \frac{4j H_{\nu}^{(1)}(k_0 \rho) \left\{ e^{j\nu[\phi - \frac{3\pi}{2} + (2m+1)\pi]} + e^{-j\nu[\phi - \frac{\pi}{2} - (2m+1)\pi]} \right\}}{\pi \beta [H_{\nu}^{(1)}(\beta)]^2 \frac{\partial}{\partial \nu} \left([1\beta] + \frac{n}{\mu_r} [1(|n|\beta)] \right)} \Big|_{\nu=\nu_q} \quad (36)
\end{aligned}$$

The exponential dependences of the residue series in (36) and the residue series in (30) are analogous to each other. Hence, the convergence region of the residue series in (36) and the one in (30) are identical. The geometrical shadow regions corresponding to the first term of the Debye series for the double positive and double negative cylinders are the same.

The residue series representations in (30) and (36) are valid in the geometrical shadow region. Outside the geometrical shadow region, for $m = 0$, the residue series does not converge because the scattered field is not formed by the creeping waves on the surface of the dielectric cylinder. The geometrically lit region is one of the regions where the residue series does not converge for $m = 0$. In the geometrically lit region, the scattered field for $m = 0$ is due to the rays reflected by the dielectric cylinder. The steepest descent method (SDM) representation of the scattering integral is useful for obtaining the field due to reflected or transmitted rays. Hence, the scattered field in this region can be calculated by the SDM.

The integral to be computed in the geometrically lit region is given as follows

$$\begin{aligned}
& \frac{1}{2} \left\{ \int_{-\infty+j\varepsilon}^{\infty+j\varepsilon} \left[\frac{R_{22} H_{\nu}^{(2)}(\beta) H_{\nu}^{(1)}(k_0 \rho) + H_{\nu}^{(1)}(\beta) H_{\nu}^{(2)}(k_0 \rho)}{H_{\nu}^{(1)}(\beta)} \right] \right. \\
& \quad \left. \left[e^{j\nu(\phi - \frac{\pi}{2})} + e^{-j\nu(\phi - \frac{3\pi}{2})} \right] d\nu \right\} \quad (37)
\end{aligned}$$

The integral in (37) is the term corresponding to $m = 0$ in the integral series in the first part of Equation (30). First, it is assumed that the integral in (37) can be separated into two parts. This separation is possible only if each of the parts is a convergent integral. The integral is separated in the following way:

$$\begin{aligned} & \frac{1}{2} \left\{ \int_{-\infty+j\epsilon}^{\infty+j\epsilon} \left[\frac{R_{22}H_{\nu}^{(2)}(\beta)H_{\nu}^{(1)}(k_0\rho)}{H_{\nu}^{(1)}(\beta)} \right] \left[e^{j\nu(\phi-\frac{\pi}{2})} + e^{-j\nu(\phi-\frac{3\pi}{2})} \right] d\nu \right\} \\ & + \frac{1}{2} \left\{ \int_{-\infty+j\epsilon}^{\infty+j\epsilon} H_{\nu}^{(2)}(k_0\rho) \left[e^{j\nu(\phi-\frac{\pi}{2})} + e^{-j\nu(\phi-\frac{3\pi}{2})} \right] d\nu \right\} \end{aligned} \quad (38)$$

In order to compute the first integral in (38), the Debye asymptotic expansion of the integrand must be found. The asymptotic expansion is made to convert the integrand to a form which is suitable for the ray interpretation.

The first integral in (38) is also separated into two parts assuming that each of them is convergent. The separation is as follows:

$$\begin{aligned} & \frac{1}{2} \left\{ \int_{-\infty+j\epsilon}^{\infty+j\epsilon} \left[\frac{R_{22}H_{\nu}^{(2)}(\beta)H_{\nu}^{(1)}(k_0\rho)}{H_{\nu}^{(1)}(\beta)} \right] \left[e^{j\nu(\phi-\frac{\pi}{2})} + e^{-j\nu(\phi-\frac{3\pi}{2})} \right] d\nu \right\} \\ & = \frac{1}{2} \left\{ \int_{-\infty+j\epsilon}^{\infty+j\epsilon} \left[\frac{R_{22}H_{\nu}^{(2)}(\beta)H_{\nu}^{(1)}(k_0\rho)}{H_{\nu}^{(1)}(\beta)} \right] e^{j\nu(\phi-\frac{\pi}{2})} d\nu \right\} \\ & + \frac{1}{2} \left\{ \int_{-\infty+j\epsilon}^{\infty+j\epsilon} \left[\frac{R_{22}H_{\nu}^{(2)}(\beta)H_{\nu}^{(1)}(k_0\rho)}{H_{\nu}^{(1)}(\beta)} \right] e^{-j\nu(\phi-\frac{3\pi}{2})} d\nu \right\} \end{aligned} \quad (39)$$

After the Debye asymptotic form of the integrand of the first integral in (39) is obtained and the first derivative of the exponential part of the integrand is taken, the following equation is found for the saddle point $\bar{\nu}$:

$$2 \cos^{-1} \left(\frac{\bar{\nu}}{\beta} \right) - \cos^{-1} \left(\frac{\bar{\nu}}{k_0\rho} \right) + \phi - \frac{\pi}{2} = 0 \quad (40)$$

In order to solve the equation in (40), the following definitions are

employed:

$$\left. \begin{aligned} \bar{v} &= \beta \sin(w) \\ x &= \cos^{-1} \left(\frac{\bar{v}}{k_0 \rho} \right) \quad \text{for } 0 < x < \frac{\pi}{2} \end{aligned} \right\} \quad (41)$$

The solution of Equation (40) is given as

$$x = \frac{\pi}{2} - 2w + \phi \quad (42)$$

Letting

$$w = \theta \quad (43)$$

matches the physical picture in Fig. 7 with the relation in (42). In a similar way, it can be shown in terms of the exponential dependence that the second integral in (39) denotes the field at the point $F(\rho, -\phi)$ due to the ray which is incident on the point $P(a, -\theta)$ and is reflected by the cylinder to the field point $F(\rho, -\phi)$. The geometrically lit region of the double negative cylinder corresponding to the first term of the

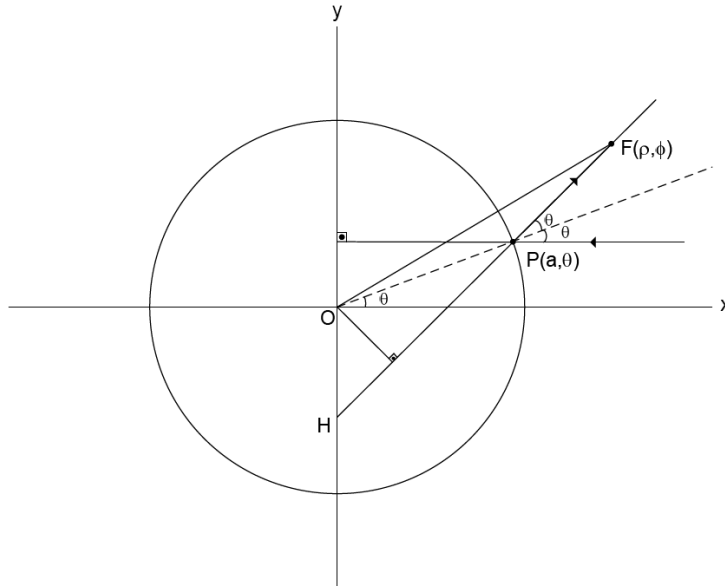


Figure 7. The physical interpretation for the geometrically lit region of the double positive cylinder corresponding to the first term of the Debye series.

Debye series is the same as that of the double positive cylinder. In the double negative cylinder case, the same physical interpretation is valid for the geometrically lit region corresponding to the first term of the Debye series.

6. THE SECOND TERM OF THE DEBYE EXPANSION

The contribution of the second term of the Debye expansion to the scattered field is obtained by inserting the expression in (22) with p being equal to 1 and with the subscript changed to ν into the place of x_ν in the scattered field integral in (24). After some operations on the integrand and setting m to 0, the following expression is obtained for the contribution of the second term of the Debye expansion to the scattered field:

$$\begin{aligned}
 E_s^{second\ term} = & \frac{1}{2} \int_{-\infty+j\varepsilon}^{\infty+j\varepsilon} H_\nu^{(1)}(k_0\rho) \frac{H_\nu^{(2)}(\beta) H_\nu^{(1)}(\alpha)}{H_\nu^{(1)}(\beta) H_\nu^{(2)}(\alpha)} T_{12}T_{21} e^{j\nu(\phi+\frac{3\pi}{2})} d\nu \\
 & + \frac{1}{2} \int_{-\infty+j\varepsilon}^{\infty+j\varepsilon} H_\nu^{(1)}(k_0\rho) \frac{H_\nu^{(2)}(\beta) H_\nu^{(1)}(\alpha)}{H_\nu^{(1)}(\beta) H_\nu^{(2)}(\alpha)} T_{12}T_{21} e^{j\nu(-\phi+\frac{3\pi}{2})} d\nu
 \end{aligned} \tag{44}$$

The integral is separated into two parts with the assumption that each of the two parts is convergent. This assumption is automatically verified when the integrals are calculated. The second term of the Debye expansion represents the scattered field due to the rays which are transmitted into the cylinder and then transmitted out of the cylinder to form the scattered field at the field point. These rays also have their own geometrically lit and geometrical shadow regions. The geometrically lit region of the double positive cylinder for the ρ coordinate of ρ_0 , $n > \sqrt{2}$ and corresponding to the second term of the Debye series is the shaded region shown in Fig. 8.

The scattered field due to the second term of the Debye series is expressed as follows when the integral in (44) is calculated using the Cauchy integral formula:

$$E_s^{second\ term} = \left[-\frac{16\pi j}{(\pi\beta)^2} \right] \sum_l \left\{ \frac{f'(\nu)}{[g(\nu)]^2} - \frac{2f(\nu)g'(\nu)}{[g(\nu)]^3} \right\} \Big|_{\nu \rightarrow \nu_l} \tag{45}$$

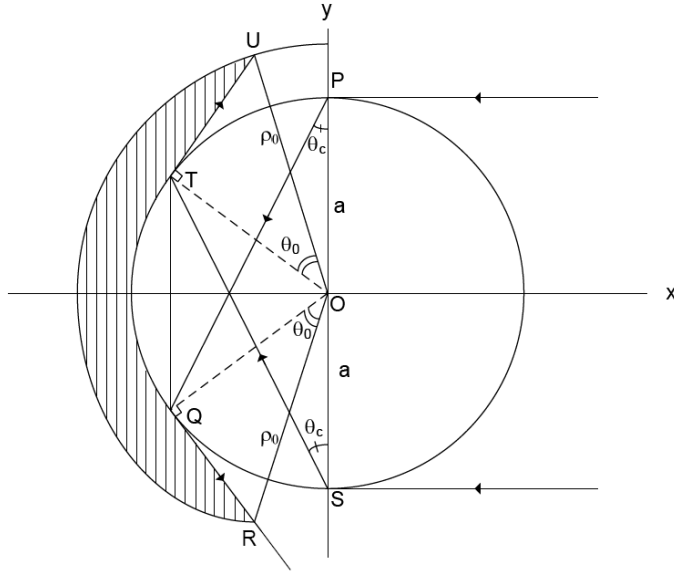


Figure 8. The geometrically lit region of the double positive cylinder for the ρ coordinate of ρ_0 , $n > \sqrt{2}$ and corresponding to the second term of the Debye series.

where

$$f(\nu) \triangleq \left. \begin{aligned} & [1\beta] - \frac{n}{\mu_r} [2\alpha] \triangleq g(\nu)(\nu - \nu_1) \\ & \frac{H_\nu^{(1)}(k_0\rho) \left[e^{j\nu(\phi + \frac{3\pi}{2})} + e^{j\nu(-\phi + \frac{3\pi}{2})} \right]}{[H_\nu^{(1)}(\beta)H_\nu^{(2)}(\alpha)]^2} \end{aligned} \right\} \quad (46)$$

If Equation (45) is explicitly written, then it can be seen that

$$\frac{H_\nu^{(1)}(k_0\rho)}{[H_\nu^{(2)}(\alpha)]^2} \left[e^{j\nu(\phi + \frac{3\pi}{2})} + e^{j\nu(-\phi + \frac{3\pi}{2})} \right] \quad (47)$$

can be fixed as a common factor. In order to determine the convergence region of the residue series and relate it to the physical picture of the surface waves creeping on the cylinder from the geometrically lit region to the geometrical shadow region, the Debye asymptotic expansion is applied to the Hankel functions in the common factor. Then, the common factor takes the following form with only the exponential

terms shown:

$$e^{\left\{j\left[\left((k_0\rho)^2-\nu^2\right)^{\frac{1}{2}}+2(\alpha^2-\nu^2)^{\frac{1}{2}}\right]\right\}} e^{\left\{j\left[-\nu\cos^{-1}\left(\frac{\nu}{k_0\rho}\right)-2\nu\cos^{-1}\left(\frac{\nu}{\alpha}\right)\right]\right\}} \left[e^{j\nu\left(\phi+\frac{3\pi}{2}\right)} + e^{j\nu\left(-\phi+\frac{3\pi}{2}\right)} \right] \quad (48)$$

Since the poles are close to β , they can be approximated to be equal to β in the first exponential factor in (48). In addition, the following equality and the definitions

$$\left. \begin{aligned} \cos^{-1}(t) &= \frac{\pi}{2} - \sin^{-1}(t) \\ \theta_0 &= \cos^{-1}\left(\frac{a}{\rho}\right) \\ \theta_c &= \sin^{-1}\left(\frac{1}{n}\right) \end{aligned} \right\} \quad (49)$$

are used in Equation (48) to obtain the common factor in the following form:

$$e^{\left\{j\left[\left((k_0\rho)^2-\beta^2\right)^{\frac{1}{2}}+2(\alpha^2-\beta^2)^{\frac{1}{2}}\right]\right\}} e^{[j\nu(-\theta_0+2\theta_c-\pi)]} e^{j\nu\left(\phi+\frac{3\pi}{2}\right)} + e^{\left\{j\left[\left((k_0\rho)^2-\beta^2\right)^{\frac{1}{2}}+2(\alpha^2-\beta^2)^{\frac{1}{2}}\right]\right\}} e^{[j\nu(-\theta_0+2\theta_c-\pi)]} e^{j\nu\left(-\phi+\frac{3\pi}{2}\right)} \quad (50)$$

For the convergence of the residue series, the exponentials in the expression (50) must converge. Keeping in mind that the imaginary parts of the poles are positive, convergence is possible only if the following conditions are both satisfied:

$$\left. \begin{aligned} -\theta_0 + 2\theta_c + \phi + \frac{\pi}{2} &> 0 \\ -\theta_0 + 2\theta_c - \phi + \frac{\pi}{2} &> 0 \end{aligned} \right\} \quad (51)$$

The satisfaction of both of the conditions requires the following range of convergence of the residue series:

$$\theta_0 - 2\theta_c - \frac{\pi}{2} < \phi < -\theta_0 + 2\theta_c + \frac{\pi}{2} \quad (52)$$

If Fig. 8 is revisited, it can be seen that the above range is the geometrical shadow of the double positive cylinder for the second term of the Debye series.

The counterpart of the integral in Equation (45) for the double negative cylinder is given as follows:

$$E_s^{second\ term} = \left[-\frac{16\pi j}{(\pi\beta)^2} \right] \sum_l \text{Res} \left\{ \frac{[f(\nu)/[g(\nu)]^2]}{(\nu - \nu_l)^2} \right\} \Big|_{\nu \rightarrow \nu_l} \quad (53)$$

where

$$f(\nu) \triangleq \frac{[1\beta] + \frac{n}{\mu_r}[1\alpha] \triangleq g(\nu)(\nu - \nu_l)}{[H_\nu^{(1)}(\beta)H_\nu^{(1)}(|n|\beta)]^2} \left[e^{j\nu(\phi - \frac{\pi}{2})} + e^{j\nu(-\phi - \frac{\pi}{2})} \right] \quad (54)$$

After the residue series is written explicitly, it can be seen that the following expression can be fixed as a common factor:

$$\frac{H_\nu^{(1)}(k_0\rho)}{[H_\nu^{(1)}(|n|\beta)]^2} \left[e^{j\nu(\phi - \frac{\pi}{2})} + e^{j\nu(-\phi - \frac{\pi}{2})} \right] \quad (55)$$

The Debye asymptotic expansion is applied to the common factor to determine the convergence region of the residue series in a more detailed manner. The exponential part of the Debye asymptotic expansion of the common factor is given as follows:

$$e^{\left\{ j \left[((k_0\rho)^2 - \nu^2)^{\frac{1}{2}} - 2(|n|^2\beta^2 - \nu^2)^{\frac{1}{2}} \right] \right\}} e^{\left\{ j \left[-\nu \cos^{-1} \left(\frac{\nu}{k_0\rho} \right) + 2\nu \cos^{-1} \left(\frac{\nu}{|n|\beta} \right) \right] \right\}} \left[e^{j\nu(\phi - \frac{\pi}{2})} + e^{j\nu(-\phi - \frac{\pi}{2})} \right] \quad (56)$$

The poles in Equation (53) are close to β . Hence, the poles are approximated by β in the first factor in Equation (56). The definitions in (49) with n replaced with $|n|$ are made to write the common factor in the following more compact form:

$$e^{\left\{ j \left[((k_0\rho)^2 - \beta^2)^{\frac{1}{2}} - 2\beta(|n|^2 - 1)^{\frac{1}{2}} \right] \right\}} e^{j\nu(-\theta_0 - 2\theta_c + \phi + \frac{\pi}{2})} + e^{\left\{ j \left[((k_0\rho)^2 - \beta^2)^{\frac{1}{2}} - 2\beta(|n|^2 - 1)^{\frac{1}{2}} \right] \right\}} e^{j\nu(-\theta_0 - 2\theta_c - \phi + \frac{\pi}{2})} \quad (57)$$

Since the poles are in the upper half of the complex ν -plane, the common factor converges provided the following conditions are satisfied:

$$\left. \begin{aligned} -\theta_0 - 2\theta_c + \phi + \frac{\pi}{2} &> 0 \\ -\theta_0 - 2\theta_c - \phi + \frac{\pi}{2} &> 0 \end{aligned} \right\} \quad (58)$$

The satisfaction of both of the conditions in Equation (58) requires the following range of ϕ for the convergence of the residue series:

$$\theta_0 + 2\theta_c - \frac{\pi}{2} < \phi < -\theta_0 - 2\theta_c + \frac{\pi}{2} \quad (59)$$

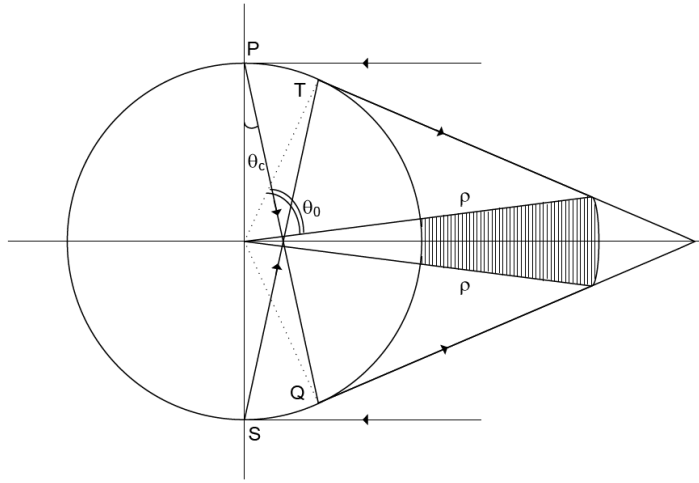


Figure 9. The geometrical shadow region of the double negative cylinder corresponding to the second term of the Debye series is the shaded region for $|n| > \sqrt{2}$.

In Fig. 9, the geometrical shadow region of the double negative cylinder corresponding to the second term of the Debye series is shown. When the geometrical shadow region of the double negative cylinder corresponding to the second term of the Debye series is compared to that of the double positive cylinder corresponding to the second term of the Debye series for $|n| > \sqrt{2}$, it can be observed that the double negative cylinder has a quite smaller geometric shadow region. For $1 < |n| < \sqrt{2}$, the double positive cylinder has a quite smaller geometrical shadow region corresponding to the second term of the Debye series.

It is now time to analyze the geometrically lit region of the double positive cylinder corresponding to the second term of the Debye series. After the Debye asymptotic expansion of the second integrand in (44) is carried out and the derivative of the exponential part with respect to ν is evaluated, the following steepest descent equation for the saddle point is obtained:

$$2 \cos^{-1} \left(\frac{\bar{\nu}}{\beta} \right) - \cos^{-1} \left(\frac{\bar{\nu}}{k_0 \rho} \right) - 2 \cos^{-1} \left(\frac{\bar{\nu}}{\alpha} \right) - \phi + \frac{3\pi}{2} = 0 \quad (60)$$

The following change of variable is performed:

$$\bar{\nu} \triangleq \beta \cos(w) \quad (61)$$

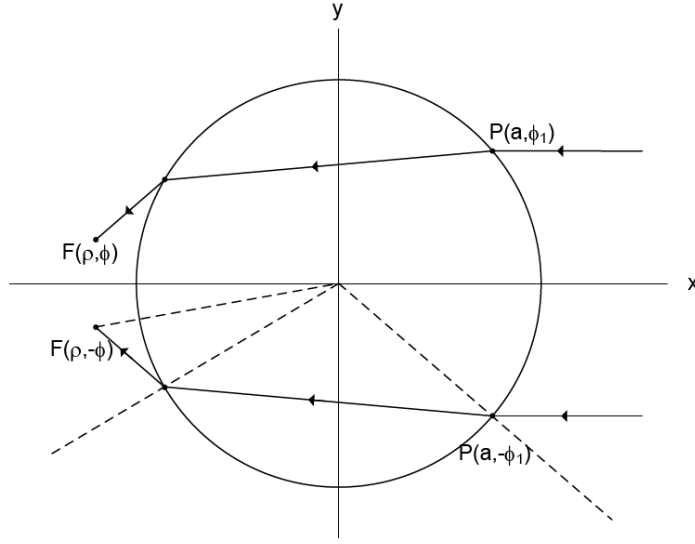


Figure 10. The physical picture for the second term of the Debye series in the geometrically lit region of the double positive cylinder.

Then, the steepest descent equation takes the following form:

$$2w - \cos^{-1} \left[\frac{a}{\rho} \cos(w) \right] - 2 \cos^{-1} \left[\frac{1}{n} \cos(w) \right] - \phi + \frac{3\pi}{2} = 0 \quad (62)$$

In order to establish the relation between the steepest descent equation and the physical picture for the second term of the Debye expansion, the expected physical picture is first drawn in Fig. 10 and the mathematical expression for it is derived. Then, it will be observed that the steepest descent equation and the derived mathematical expression are the same.

From Fig. 10, the following equation can be derived:

$$2 \sin^{-1} \left[\frac{1}{n} \sin(\phi_1) \right] - 2\phi_1 + \sin^{-1} \left[\frac{a}{\rho} \sin(\phi_1) \right] = \phi - \pi \quad (63)$$

The following substitutions are to be made in Equation (63):

$$\left. \begin{aligned} \phi_1 &= \frac{\pi}{2} - x \\ \sin^{-1}(t) &= \frac{\pi}{2} - \cos^{-1}(t) \end{aligned} \right\} \quad (64)$$

Then, Equation (63) takes the following form:

$$2x - \cos^{-1} \left[\frac{a}{\rho} \cos(x) \right] - 2 \cos^{-1} \left[\frac{1}{n} \cos(x) \right] - \phi + \frac{3\pi}{2} = 0 \quad (65)$$

If Equations (62) and (65) are compared, it can easily be seen that they become identical if the following equation is written for w :

$$w = x \quad (66)$$

Using the first part of Equation (64), Equation (66) can be written as follows:

$$w = \frac{\pi}{2} - \phi_1 \quad (67)$$

Equation (67) gives the solution for the saddle point equation in order to match the steepest descent equation to the physical picture. For the geometrically lit region corresponding to the second term of the Debye series in the case of the double negative cylinder, the differences in the calculations arise from the negativity of the refractive index which shows itself in the following relation:

$$\alpha = -|n|\beta \quad (68)$$

The Debye asymptotic approximation is applied to the integrand of the second integral in (44). In applying the Debye asymptotic approximation to the Hankel functions with the argument α , the following analytical continuity relations are used from [44]:

$$\left. \begin{aligned} H_\nu^{(1)}(ze^{j\pi}) &= -e^{-j\nu\pi} H_\nu^{(2)}(z) \\ H_\nu^{(2)}(ze^{-j\pi}) &= -e^{j\nu\pi} H_\nu^{(1)}(z) \end{aligned} \right\} \quad (69)$$

After the application of the Debye asymptotic approximation with the analytical continuity relations, the first derivative of the exponent of the integrand with respect to ν is taken and the resulting expression is equated to zero to find the possible saddle point $\bar{\nu}$ as follows:

$$2 \cos^{-1} \left(\frac{\bar{\nu}}{\beta} \right) + 2 \cos^{-1} \left(\frac{\bar{\nu}}{|n|\beta} \right) - \cos^{-1} \left(\frac{\bar{\nu}}{k_0\rho} \right) - \phi - \frac{\pi}{2} = 0 \quad (70)$$

The physical picture for the double negative cylinder is the same as the double positive medium except the negative refraction in the case of the double negative cylinder. The physical picture for the case of

the double negative cylinder is shown in Fig. 11. From Fig. 11, the following relation can be derived:

$$-2 \sin^{-1} \left(\frac{1}{|n|} \sin \theta_1 \right) + \sin^{-1} \left(\frac{a}{\rho} \sin \theta_1 \right) - 2\theta_1 - \phi + \pi = 0 \quad (71)$$

The following definition and relation are used to match the equation in (70) to the one in (71):

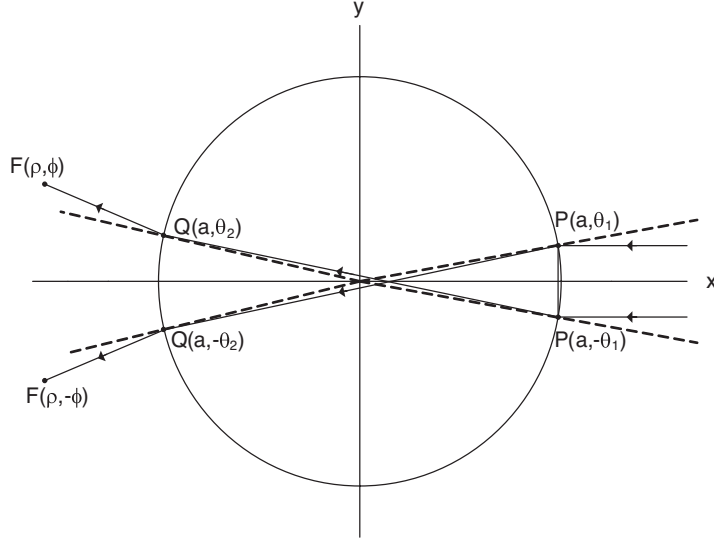


Figure 11. The physical picture in the geometrically lit region of the double negative cylinder corresponding to the second term of the Debye series.

$$\left. \begin{aligned} \bar{\nu} &= \beta \cos w \\ \sin^{-1} x &= \frac{\pi}{2} - \cos^{-1} x \end{aligned} \right\} \quad (72)$$

Equation (70) and Equation (71) become identical when the solution for the saddle point is written as follows:

$$w = \frac{\pi}{2} - \theta_1 \quad (73)$$

7. NUMERICAL RESULTS

In this section, the series results which are computed using Mathematica and correspond to the first and second terms of the Debye

series expansions of the scattered field are compared with the same series results obtained using the residue series and the steepest descent method. The calculations are made for the geometrical shadow and the geometrically lit regions of the first and second terms of the Debye series for the scattering by the infinitely long double negative cylinder. Our main concern is to provide a comparison between some analytical (or semi-analytical) results obtained by means of different approaches. In order to be able to compare these approaches properly, we prefer to present our results (which are very close to each other in several cases) in tables, rather than in graphical form. Throughout the tabulation of the results, the following definition is used for the percentage errors in the results:

$$\text{percentage error in the result} \triangleq \frac{|\text{result} - \text{Debye series result}|}{\text{Debye series result}} \times 100 \quad (74)$$

The contribution of the first term of the Debye series to the field in the geometrical shadow of the double negative cylinder corresponding to the first term of the Debye series is denoted by the following series expression:

$$\sum_{l=-\infty}^{\infty} \frac{1}{2} j^{-l} \left[R_{22}(l) \frac{H_l^{(2)}(\beta)}{H_l^{(1)}(\beta)} H_l^{(1)}(k_0 \rho) + H_l^{(2)}(k_0 \rho) \right] e^{-jl\phi} \quad (75)$$

The series in the expression (75) is computed using Mathematica. The integral corresponding to the series in (75) is calculated using the residue series. In the calculation of the residue series, only three terms of the series corresponding to first three poles of the integrand are used to obtain the results shown in the tables. The computational advantage is obvious. The residue series results are obtained without using the Debye expansion for $H_\nu^{(1)}(k_0 \rho)$ in the residue series. The following parameters are used in the calculations:

$$\begin{aligned} \beta &= 50\pi \\ \mu_r &= -1 \\ k_0 \rho &= 3 \left(\beta + \beta^{\frac{1}{3}} \right) \end{aligned}$$

The tabulation of the results are given in the Tables 1–3.

The contribution of the second term of the Debye series to the corresponding geometrical shadow region of the double negative

Table 1. The series results of the double negative cylinder with respect to n , geometrical shadow region of the first term of the Debye series.

n	161.2°	164.96°	168.72°
-1.5	-0.379787+0.172141j	0.0690321+0.145803j	0.057261-0.0487625j
-3	-0.370295+0.175864j	0.0683862+0.138669j	0.0518655-0.0458897j
-5	-0.367705+0.176887j	0.0682042+0.136741j	0.0504828-0.0451287j
n	172.48°	176.24°	180°
-1.5	-0.0357022-0.0132994j	-0.00607961+0.0153692j	0.0227744-0.00735572j
-3	-0.0317714-0.0119036j	-0.00479248+0.0136177j	0.0188184-0.00634356j
-5	-0.0307807-0.0115351j	-0.00448488+0.0131663j	0.0178605-0.00608991j

Table 2. The residue series results of the double negative cylinder with respect to n , geometrical shadow region of the first term of the Debye series.

n	161.2°	164.96°	168.72°
-1.5	-0.299356+0.074339j	0.0633379+0.127624j	0.0542479-0.0490218j
-3	-0.295446+0.0772575j	0.0622797+0.121706j	0.049105-0.0460048j
-5	-0.294361+0.0781634j	0.0620119+0.120103j	0.047789-0.0452116j
n	172.48°	176.24°	180°
-1.5	-0.0358987-0.0128224j	-0.00600752+0.0154229j	0.0228018-0.00737693j
-3	-0.0319246-0.0114758j	-0.00472903+0.0136604j	0.0188398-0.00636206j
-5	-0.030924-0.0111203j	-0.00442373+0.0132065j	0.0178805-0.00610766j

cylinder is represented by the following series:

$$\sum_{l=-\infty}^{\infty} 0.5j^{-l} T_{12}(l) T_{21}(l) \frac{H_l^{(2)}(\beta) H_l^{(2)}(|n\beta|)}{H_l^{(1)}(\beta) H_l^{(1)}(|n\beta|)} H_l^{(1)}(k_0 \rho) e^{-jl\phi} \quad (76)$$

The series is computed in the geometrical shadow region corresponding to the second term of the Debye series using Mathematica and is compared to the residue series result. The residue series computation is carried out by using only three terms of the series corresponding

Table 3. The percentage errors in the magnitudes of the residue series results of the double negative cylinder with respect to n , geometrical shadow region of the first term of the Debye series.

n	161.2°	164.96°	168.72°
-1.5	26.0277082	11.68043921	2.784514192
-3	25.50517893	11.57679535	2.835851408
-5	25.35965865	11.54363599	2.845602239
n	172.48°	176.24°	180°
-1.5	0.055425729	0.143061852	0.136195848
-3	0.010576374	0.13441283	0.131887027
-5	0.02569378	0.133119844	0.130687912

to first three poles of the integrand of the integral calculated by the residue series. The Debye approximation is not employed in the residue series computations. Since the geometrical shadow region of the second term of the Debye series for the double negative cylinder is very small compared to that of the double positive cylinder for $|n| > \sqrt{2}$, the tabulation parameters are chosen as follows:

$$\begin{aligned}\beta &= 50\pi \\ \mu_r &= -1 \\ k_0\rho &= 1.4 \left(\beta + \beta^{\frac{1}{3}} \right)\end{aligned}$$

The tabulation of the results are given in the Tables 4–5.

The contribution of the first term of the Debye series to the corresponding geometrically lit region of the double negative cylinder is denoted by the following series expression:

$$\sum_{l=-\infty}^{\infty} \frac{1}{2} j^{-l} \left[R_{22}(l) \frac{H_l^{(2)}(\beta)}{H_l^{(1)}(\beta)} - 1 \right] H_l^{(1)}(k_0\rho) e^{-jl\phi} \quad (77)$$

The integral corresponding to the series is calculated using the steepest descent method. However, only the upper half of the steepest descent path is traversed since the integrand blows up in the lower half of the ν -plane. This causes a factor of $\frac{1}{2}$ to be put in front of the steepest

Table 4. The residue series results of the double negative cylinder for $n = -4$, geometrical shadow region of the second term of the Debye series.

	-14.7198°	-11.7759°	-8.8319°
Series	0.0142191-0.00801176j	0.00251608+0.0110614j	-0.011142-0.00121268j
Residue series without the Debye approximation	0.0105111-0.00156402j	0.00216606+0.00880508j	-0.0106298-0.000738343j
Percentage error in the magnitude of the residue series	34.88816713	20.06671016	4.928596897
	-5.88794°	-2.94397°	0°
Series	0.0058922-0.00463913j	0.00397166+0.00176787j	-0.00845512+0.00118164j
Residue series without the Debye approximation	0.00568141-0.00465546j	0.00402406+0.0017269j	-0.00846816+0.0012186j
Percentage error in the magnitude of the residue series	2.055113714	0.726995125	0.212021275

Table 5. The residue series results of the double negative cylinder for $n = -5$, geometrical shadow region of the second term of the Debye series.

	-20.6009°	-16.4808°	-12.3606°
Series	-0.00946064-0.00792567j	-0.00823302+0.00339752j	-0.00143224+0.00634083j
Residue series without the Debye approximation	-0.0046831-0.00750296j	-0.00734266+0.00318733j	-0.00128335+0.00625093j
Percentage error in the magnitude of the residue series	28.33671668	10.12624735	1.834643857
	-8.24038°	-4.12019°	0°
Series	0.0022886+0.00279095j	0.00209926-0.00154353j	0.00139885-0.00326749j
Residue series without the Debye approximation	0.00231037+0.00276613j	0.00210171-0.00154947j	0.00139907-0.00326984j
Percentage error in the magnitude of the residue series	0.14521514	0.210877984	0.06321885

Table 6. The series results of the double negative cylinder with respect to n , the geometrically lit region of the first term of the Debye series.

n	0°	5°	10°
-1.5	0.0774171+0.0411237j	0.0582661+0.0656221j	-0.0295278+0.0829418j
-3	0.194277+0.101381j	0.14672+0.162826j	-0.0720361+0.207125j
-5	0.259111+0.135031j	0.195676+0.216914j	-0.0957583+0.275822j
n	15°	20°	
-1.5	-0.0755711-0.0460884j	0.0885957-0.010217j	
-3	-0.188213-0.112912j	0.218105-0.0267571j	
-5	-0.250221-0.149926j	0.289121-0.0356253j	

Table 7. The SDM results for the double negative cylinder with respect to n , the geometrically lit region of the first term of the Debye series.

n	0°	5°	10°
-1.5	0.0773859+0.0411803j	0.058217+0.0656643j	-0.0295889+0.0829189j
-3	0.194329+0.101277j	0.146806+0.162745j	-0.0719181+0.207163j
-5	0.259247+0.134761j	0.1959+0.216707j	-0.0954595+0.275921j
n	15°	20°	
-1.5	-0.0755357-0.0461439j	0.0886019-0.0101506j	
-3	-0.18828-0.112794j	0.218083-0.0269062j	
-5	-0.250387-0.14964j	0.289072-0.0359769j	

descent result. The following parameters are used in the calculations:

$$\begin{aligned} \beta &= 50\pi \\ \mu_r &= -1 \\ k_0\rho &= 3\left(\beta + \beta^{\frac{1}{3}}\right) \end{aligned}$$

The tabulation of the results are given in Tables 6–8.

Table 8. The percentage errors in the magnitudes of the SDM results of the double negative cylinder with respect to n , the geometrically lit region of the first term of the Debye series.

n	0°	5°	10°
-1.5	0.001115536	0.001162385	0.001200975
-3	0.000904721	0.001174067	0.001293055
-5	0.001374673	0.001199037	0.001474144
n	15°	20°	
-1.5	0.001469597	0.001595416	
-3	0.00146169	0.001651576	
-5	0.001513114	0.001859621	

Table 9. The series results of the double negative cylinder with respect to n , the geometrically lit region of the second term of the Debye series.

n	161.2°	164.96°	168.72°
-1.5	-0.0439222+0.310061j	0.239372+0.202416j	0.312637-0.0262297j
-3	-0.222489+0.163j	0.096654+0.259189j	0.271431+0.0565408j
-5	-0.212743+0.0367327j	0.0131297+0.21654j	0.202784+0.0793392j
n	172.48°	176.24°	180°
-1.5	0.250831-0.188751j	0.174388-0.261152j	0.144033-0.279086j
-3	0.241623-0.136895j	0.162109-0.225817j	0.128001-0.246857j
-5	0.19752-0.0930337j	0.13102-0.175087j	0.100967-0.194109j

The contribution of the second term of the Debye series to the corresponding geometrically lit region of the double negative cylinder is calculated both by using the series expression and by the saddle point method (SDM). The computed series is given by the following expression:

$$\sum_{l=-\infty}^{\infty} 0.5j^{-l} T_{12}(l) T_{21}(l) \frac{H_l^{(2)}(\beta) H_l^{(2)}(|n|\beta)}{H_l^{(1)}(\beta) H_l^{(1)}(|n|\beta)} H_l^{(1)}(k_0 \rho) e^{-jl\phi} \quad (78)$$

The integral corresponding to the series is calculated using the SDM. The integrand of the integral does not vanish as $|\nu| \rightarrow \infty$ in the lower

half of the plane. Hence, only the upper part of the steepest descent path contributes to the integral. This causes a $\frac{1}{2}$ factor to be put in front of the SDM result of the integral. The following parameters are

Table 10. The SDM results of the double negative cylinder with respect to n , the geometrically lit region of the second term of the Debye series.

n	161.2°	164.96°	168.72°
-1.5	-0.0430699+0.31018j	0.239922+0.201764j	0.312565-0.0270754j
-3	-0.222029+0.163623j	0.0973704+0.258919j	0.271583+0.0557978j
-5	-0.212627+0.0373855j	0.0137826+0.216497j	0.203016+0.078735j
n	172.48°	176.24°	180°
-1.5	0.250322-0.189427j	0.173686-0.26162j	0.143283-0.279471j
-3	0.24125-0.137549j	0.161498-0.226252j	0.127335-0.2472j
-5	0.197243-0.0936136j	0.130506-0.175468j	0.100399-0.194401j

Table 11. The percentage errors in the magnitudes of the SDM results of the double negative cylinder with respect to n , the geometrically lit region of the second term of the Debye series.

n	161.2°	164.96°	168.72°
-1.5	0.000170643	4.39294E-05	3.33126E-05
-3	0.000652129	0.000581594	0.00060455
-5	0.001028306	0.001115079	0.00143711
n	172.48°	176.24°	180°
-1.5	0.000284875	0.000156852	0.000224341
-3	0.000405367	0.000694855	0.000382958
-5	0.001166983	0.000902219	0.000972343

used in the calculations:

$$\begin{aligned}\beta &= 50\pi \\ \mu_r &= -1 \\ k_0\rho &= 3\left(\beta + \beta^{\frac{1}{3}}\right)\end{aligned}$$

The tabulations are given in Tables 9–11.

8. CONCLUSION

The modified Watson transform with the Debye expansion is a very powerful method to obtain a rapidly converging solution to the high frequency plane wave scattering by an infinitely long dielectric cylinder and to develop a physical insight related to the scattering mechanism. The geometrical shadow and the geometrically lit regions of the double positive and double negative cylinders corresponding to the first two terms of the Debye expansions are compared with each other. It is observed that the geometrically lit and geometrical shadow regions of the first term do not differ. However, the geometrically lit and geometrically shadow regions of the second term differ very much from each other. In the case of the double negative cylinder, for the refractive indices with magnitudes greater than $\sqrt{2}$, the geometrical shadow region of the second term of the Debye series is quite smaller compared to that of the double positive cylinder. Numerical simulations show that the physical insight to the scattering mechanism provided by the Debye expansion is very accurate. In addition, they are in conformity with the observations that a double negative material is a negative refractive index material and at the surface of the double negative cylinder, negative refraction occurs.

REFERENCES

1. Veselago, V. G., “The electrodynamics of substances with simultaneously negative values of ε and μ ,” *Soviet Physics Uspekhi*, Vol. 10, No. 4, January–February 1968.
2. Pendry, J. B., A. J. Hold, D. J. Robbins, and W. J. Stewart, “Magnetism from conductors and enhanced nonlinear phenomena,” *IEEE Transactions on Microwave Theory and Techniques*, Vol. 47, 2075–2084, Nov. 1999.
3. Pendry, J. B., A. J. Holden, W. J. Stewart, and I. Youngs, “Extremely low frequency plasmons in metallic mesostructures,” *Physical Review Letters*, Vol. 76, 4773, June 17, 1996.

4. Smith, D. R., W. J. Padilla, D. C. Vier, S. C. Nemat-Nasser, and S. Schultz, "Composite medium with simultaneously negative permeability and permittivity," *Physical Review Letters*, Vol. 84, 4184, May 1, 2000.
5. Pendry, J. B., "Negative refraction makes a perfect lens," *Physical Review Letters*, Vol. 85, No. 18, October 2000.
6. Shelby, R. A., D. R. Smith, and S. Schultz, "Experimental verification of a negative index of refraction," *Science*, Vol. 292, 77–79, April 6, 2001.
7. Ziolkowski, R. W. and E. Heyman, "Wave propagation in media having negative permittivity and permeability," *Physical Review E*, Vol. 64, No 056625, 2001.
8. Ziolkowski, R. W. and A. D. Kipple, "Causality and double-negative metamaterials," *Physical Review E*, Vol. 68, 026615, Part 2, 2003.
9. Caloz, C., H. Okabe, T. Iwai, and T. Itoh, "Transmission line approach of left-handed (LH) materials," *Proc. USNC/URSI National Radio Science Meeting*, Vol. 1, 39, San Antonio, TX, June 2002.
10. Grbic, A. and G. V. Eleftheriades, "A backward-wave antenna based on negative refractive index," *Proc. IEEE AP-S Int. Symp.*, Vol. 4, 340–343, San Antonio, TX, June 2002.
11. Iyer, A. K. and G. V. Eleftheriades, "Negative refractive index metamaterials supporting 2-D waves," *Proc. IEEE MTT-S Int. Symp.*, Vol. 2, 1067–1070, San Antonio, TX, June 2002.
12. Eleftheriades, G. V., A. K. Iyer, and P. C. Kramer, "Planar negative refractive index media using periodically L-C loaded transmission lines," *IEEE Transactions on Microwave Theory and Techniques*, Vol. 50, No. 12, December 2002.
13. Shelby, R. A., D. R. Smith, S. C. Nemat-Nasser, S. Schultz, "Microwave transmission through a two-dimensional, isotropic, left-handed metamaterial," *Applied Physics Letters*, Vol. 78, 489–491, 2001.
14. Pacheco Jr., J., T. M. Grzegorzczuk, B.-I. Wu, Y. Zhang, and J. A. Kong, "Power propagation in homogeneous isotropic frequency-dispersive left-handed media," *Physical Review Letters*, Vol. 89, 257401, 2002.
15. Caloz, C., C.-C. Chang, and T. Itoh, "Full-wave verification of the fundamental properties of left-handed materials in waveguide configurations," *Journal of Applied Physics*, Vol. 90, 5483–5486, 2001.

16. Ziolkowski, R. W. and A. D. Kipple, "Application of double negative materials to increase the power radiated by electrically small antennas," *IEEE Transactions on Antennas and Propagation*, Vol. 51, No. 10, October 2003.
17. Xiao, S. H., L. F. Shen, and S. L. He, "A novel directional coupler utilizing a left-handed material," *IEEE Photonics Technology Letters*, Vol. 16, No. 1, January 2004.
18. Yang, R., Y.-J. Xie, P. Wang, and L. Li, "Microstrip antennas with left-handed materials substrates," *J. of Electromagn. Waves and Appl.*, Vol. 20, No. 9, 1221–1233, 2006.
19. Zhang, J., B. Cui, J.-Z. Gu, and X.-W. Sun, "A harmonic suppressed Wilkinson power divider using complementary split ring resonators (CSRRs)," *J. of Electromagn. Waves and Appl.*, Vol. 21, No. 6, 811–819, 2007.
20. Li, Z. and T. J. Cui, "Novel waveguide directional couplers using left-handed materials," *J. of Electromagn. Waves and Appl.*, Vol. 21, No. 8, 1053–1062, 2007.
21. Guo, Y. and R. Xu, "Ultra-wideband power splitting/combining technique using zero-degree left-handed transmission lines," *J. of Electromagn. Waves and Appl.*, Vol. 21, No. 8, 1109–1118, 2007.
22. Yang, R., Y. Xie, D. Li, J. Zhang, and J. Jiang, "Bandwidth enhancement of microstrip antennas with metamaterial bilayered substrates," *J. of Electromagn. Waves and Appl.*, Vol. 21, No. 15, 2321–2330, 2007.
23. Zhang, J. and X.-W. Sun, "Harmonic suppression of branch-line and rat-race coupler using complementary split ring resonators (CSRR) cell," *Progress In Electromagnetics Research Letters*, Vol. 2, 73–79, 2008.
24. Abdalla, M. A. and Z. Hu, "On the study of left-handed coplanar waveguide coupler on ferrite substrate," *Progress In Electromagnetics Research Letters*, Vol. 1, 69–75, 2008.
25. Kuzmiak, V. and A. A. Maradudin, "Scattering properties of a cylinder fabricated from a left-handed material," *Physical Review B*, Vol. 66, 045116, 2002.
26. Ruppin, R., "Intensity distribution inside scatterers with negative-real permittivity and permeability," *Microwave and Optical Technology Letters*, Vol. 36, No. 3, February 5, 2003.
27. Wang, M. Y., J. Xu, J. Wu, Y. B. Yan, and H. L. Li, "FDTD study on scattering of metallic column covered by double-negative metamaterial," *J. of Electromagn. Waves and Appl.*, Vol. 21, No. 14, 1905–1914, 2007.

28. Valagiannopoulos, C. A., "Electromagnetic scattering from two eccentric metamaterial cylinders with frequency-dependent permittivities differing slightly each other," *Progress In Electromagnetics Research B*, Vol. 3, 23–34, 2008.
29. Hady, L. K. and A. A. Kishk, "Electromagnetic scattering from conducting circular cylinder coated by metamaterials and loaded with helical strips under oblique incidence," *Progress In Electromagnetics Research B*, Vol. 3, 189–206, 2008.
30. Oraizi, H. and A. Abdolali, "Combination of MLS, GA & CG for the reduction of RCS of multilayered cylindrical structures composed of dispersive metamaterials," *Progress In Electromagnetics Research B*, Vol. 3, 227–253, 2008.
31. Zainud-Deen, S. H., A. Z. Botrosand, and M. S. Ibrahim, "Scattering from bodies coated with metamaterial using FDFD method," *Progress In Electromagnetics Research B*, Vol. 2, 279–290, 2008.
32. Grzegorzczuk, T. M. and J. A. Kong, "Review of left-handed metamaterials: Evolution from theoretical and numerical studies to potential applications," *J. of Electromagn. Waves and Appl.*, Vol. 20, No. 14, 2053–2064, 2006.
33. Chen, B.-I. Wu, and J. A. Kong, "Review of electromagnetic theory in left-handed materials," *J. of Electromagn. Waves and Appl.*, Vol. 20, No. 15, 2137–2151, 2006.
34. Debye, P., *Physik. Z.*, Vol. 9, 775, 1908.
35. Watson, G. N., "The diffraction of electric waves by the earth," *Proceedings of the Royal Society of London*, Vol. 95, No. 666, 83–99, 1918.
36. Pumplin, J., "Application of Sommerfeld-Watson transformation to an electrostatics problem," *American Journal of Physics*, Vol. 37, No. 7, 737–739, 1969.
37. Uberall, H., "Acoustic scattering from elastic cylinders and spheres: Surface waves (Watson transform) and transmitted waves," *Diffusion et Diffraction*, Vol. 2, No. 5, 353–387, 1985.
38. Wang, H.-L., Q. Wu, X.-J. He, and L.-W. Li, "Computation of wave scattering problems from a spheric body: Derivation of the new Sommerfeld-Watson transformation," *Progress In Electromagnetics Research Symposium 2005*, 707–710, Hangzhou, China, August 22–26, 2005.
39. Valagiannopoulos, C. A., "An overview of the Watson transformation presented through a simple example," *Progress In Electromagnetics Research*, PIER 75, 137–152, 2007.

40. Inada, H., "Diffracted field computations by a series expansion," *Radio Science*, Vol. 10, 205–220, Feb. 1975.
41. Sasamori, T., T. Uno, and S. Adachi, "High-frequency analysis of electromagnetic scattering due to a dielectric cylinder," *Electronics and Communications in Japan, Part II - Electronics*, Vol. 78, No. 4, 41–55, 1995.
42. Nussenzweig, H. M., "High-frequency scattering by a transparent sphere. 1. direct reflection and transmission," *Journal of Mathematical Physics*, Vol. 10, No. 1, 82–124, Jan. 1969.
43. Nussenzweig, H. M., "High-frequency scattering by an impenetrable sphere," *Annals of Physics*, Vol. 34, 23–95, 1965.
44. Abramowitz, M. and I. A. Stegun, *Handbook of Mathematical Functions with Formulas, Graphs, and Mathematical Tables*, Dover Publications Inc., New York, 1972.